



ELSEVIER

Earth and Planetary Science Letters 156 (1998) 195–207

EPSL

Mantle plume heads and the initiation of plate tectonic reorganizations

James Todd Ratcliff^{a,*}, David Bercovici^b, Gerald Schubert^{a,c}, Loren W. Kroenke^b

^a Department of Earth and Space Sciences, University of California, Los Angeles, CA 90095-1567, USA

^b Department of Geology and Geophysics, School of Ocean and Earth Science and Technology, University of Hawaii, Honolulu, HI 96822, USA

^c Institute of Geophysics and Planetary Physics, University of California, Los Angeles, CA 90095, USA

Received 29 April 1997; revised version received 29 December 1997; accepted 14 January 1998

Abstract

We present results of numerical simulations which examine the plausibility of a reorganization of plate motions brought about by the interaction of a hot, low-viscosity plume head with the underside of a tectonic plate. A numerical model of highly viscous fluid flow driven by thermal buoyancy is employed to examine the interaction of mantle plumes with surface plates in a two-dimensional cartesian geometry. Plate-like boundary conditions applied to the upper surface consist of a large active plate with fixed speed plus a smaller passive plate whose speed and direction of motion are permitted to react to tractions induced by the underlying mantle flow (driven by the active plate). The passive plate is also subject to applied end-loads intended to simulate incipient subduction. The mantle plume is initiated with a hot patch on the lower boundary, and viscosity varies with temperature following an Arrhenius rheology. The calculations, performed with fixed aspect ratio (4×1) and fixed Rayleigh number ($Ra = 10^6$, where Ra refers to the strength of the starting plume), were found to depend on three parameters: the strength of the viscosity variation, the size of the applied end-load, and the speed of the active plate. These calculations indicate that plate motions can be sharply influenced by the lubricating effects of mantle plume heads even to the point of causing a reversal in the direction of plate motion. © 1998 Elsevier Science B.V. All rights reserved.

Keywords: mantle plumes; Pacific Plate; flood basalts; Ontong Java Plateau; plate tectonics; movement; viscosity; numerical analysis; CFD

1. Introduction

One of the more significant mysteries in geodynamics is the relationship between flood basalt events and changes in plate motion. There are enough instances in which flood basalts and plate

reorganizations are nearly simultaneous to discount their association being a coincidence [1,2]. The cause for this association necessarily depends on the origin of flood basalts. The two leading models for flood basalt formation are the following.

(1) The steady plume model [1] in which steady-state plumes feed the asthenosphere. When rifting occurs, partial melting in the plume heads results in extensive volcanism.

(2) The starting plume head model [2–4] in which the initial diapir leading a mantle plume undergoes

* Corresponding author. Present address: Jet Propulsion Laboratory, 4800 Oak Grove Dr. MS 238-332, Pasadena, CA 91109-8099, USA. Tel.: +1 (818) 354-0204; Fax: +1 (818) 393-6890; E-mail: todd.ratcliff@jp.nasa.gov

partial melting upon reaching the base of the lithosphere and engenders a flood basalt (prior to or coincident with rifting).

The first model explains how flood basalts can result from changes in plate motion (i.e., rifting leads to decompression melting) but has difficulty explaining the brevity of such events. In the steady-plume model, flood basalt events should continue as long as rifting occurs; eruptions would persist over a wide spectrum of times. However, flood basalt events are geologically brief, on the order of 2 to 3 million years. Moreover, flood basalts should occur when a ridge passes over a hotspot; no such event occurred when the Central Indian ridge migrated over the Reunion hotspot at around 40 Ma [3]. Additional arguments against the first model are summarized in [2,3,5].

The second model explains the brevity of flood basalt events and why many hotspot tracks appear to originate with such events but does not explain the coincidence of flood basalts with changes in plate motion. Plume heads form in the deep mantle and if changes in plate motion trigger (or accelerate) a Rayleigh–Taylor instability, the plume head could only reach the surface tens of millions of years after a change in plate motion [6]. With the starting-plume-head model, one needs an explanation of how the arrival of a massive plume head could trigger a change in plate motion.

Below we describe a mechanism that can offer such an explanation but first we describe the geological context in which the mechanism should be important. Recognizing the uncertainties in, and the controversy that surrounds, Pacific-wide plate reconstructions, particularly in the hotspot frame of Refs. [7–10], we offer one interpretation of a major geological event in the Cretaceous Pacific involving both flood basalts and changes in plate motion.

Prior to 122 Ma, the nascent Pacific plate was a small plate with no slabs connected to it (Fig. 1). Its motion, and likely that of the plates to the north (Izanagi and Farallon plates), was influenced by the southward motion of the Phoenix plate (based on Pacific plate motion [11,13]). The Phoenix plate was subducting beneath what is now New Zealand [14] and New Caledonia [15] (then attached to Gondwana via Australia). It is likely that the Pacific, Izanagi and Farallon plates were all being pulled to the southwest in the wake of the Phoenix plate, but at

different velocities such that their boundaries were all spreading centers with some transform motion (Fig. 1). The northern boundary of the Izanagi plate would have been undergoing compressive strike-slip motion along the margin of what is now the Japan trench; thus there seems to have been some initial convergence along the northern edge of the Izanagi plate. At around 122 Ma, the (first) Ontong-Java flood basalt event occurred after which all plate motion shifted to the northwest, following the Izanagi plate (which began subducting beneath eastern Eurasia via the Japan trench; Fig. 1) resulting in emplacements of Cretaceous rhyolites and granites in Japan [16–18]. The southward subduction of the Phoenix plate also stopped as the Phoenix plate was captured by the Pacific plate.

One explanation for these events is that prior to 124 Ma the Phoenix plate, actively moving to the southwest, induced mantle flow which dragged the northern plates after it. The ‘transpressive’ northwest motion of the Izanagi plate implies (since some convergent motion was involved) that there was incipient downwelling, i.e., forces acting to initiate northward subduction. However, the overall motion to the southwest overwhelmed these forces. When the Ontong-Java plume head arrived beneath the Pacific plate, it acted to lubricate the spreading centers around the Pacific and decouple the Pacific, Farallon, Izanagi and Japan plates from the Phoenix’s mantle traction [19]. Subduction to the northwest of the Izanagi plate could then proceed unimpeded. After decoupling, subduction of the Phoenix plate could have accelerated briefly [19], since it was no longer dragging the other plates behind it. Subsequent cessation of subduction might then be due to: (1) the slab running into the 660 km discontinuity; (2) the increased plate velocity resulting in younger, more buoyant material in the Phoenix plate thereby rendering it more gravitationally stable; or (3) collisions of continental fragments and/or oceanic plateaus (evidence of which exists in New Zealand [14]) plugging up the subduction system.

2. The decoupling model

A simple initial approach for examining the role of mantle plumes in correlation of flood basalt events

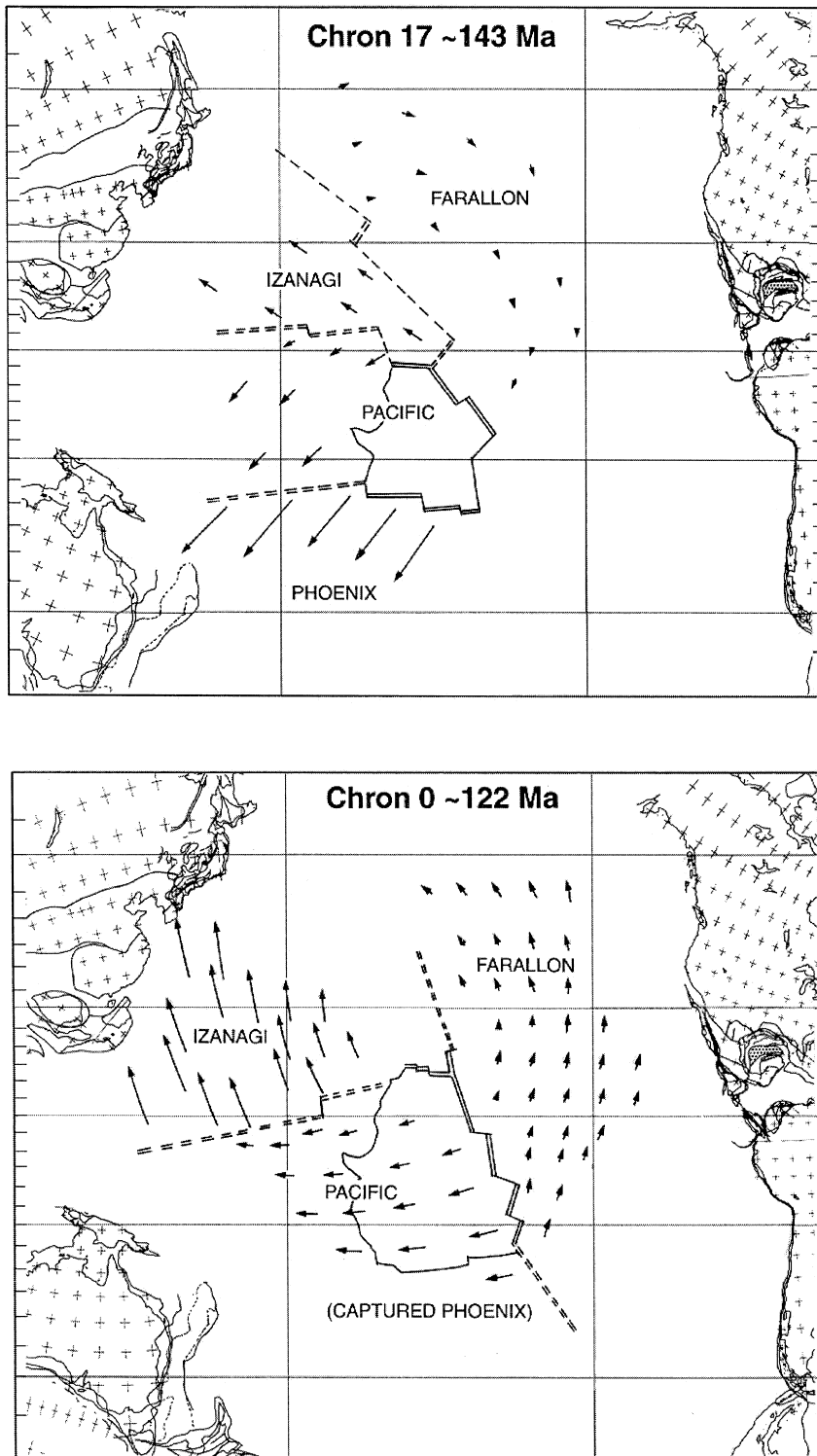


Fig. 1. Relative motions of the Phoenix, Pacific, Farallon, and Izanagi plates in the hotspot frame of Ref. [11], showing the approximate locations of the continents [12], before (top panel) and after (bottom panel) the Ontong-Java event and reorganization of plate motions.

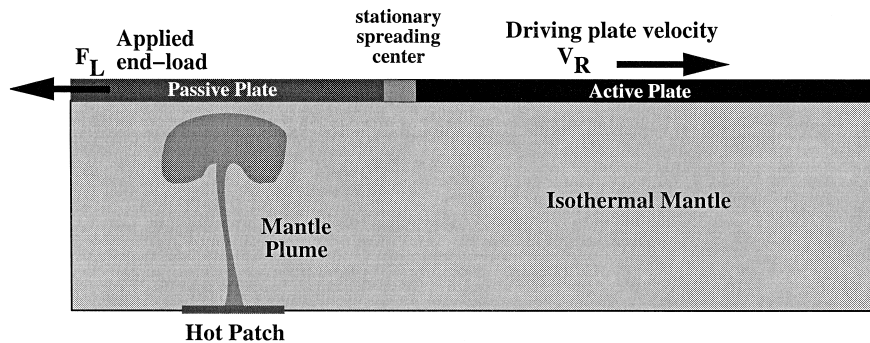


Fig. 2. Diagram of the 2D decoupling model. The salient features are the large, active-plate driving flow in an isothermal mantle, the smaller, passive plate which is free to react to mantle tractions, and the hot, low-viscosity mantle plume.

with changes in plate motion is to determine whether it is possible for a hot, low-viscosity plume head to decouple an essentially passive plate from an adjacent, actively subducting plate. Without attempting to reproduce exactly the history of the Pacific, we require that our simple model have many of the basic features of the Pacific–Phoenix system around the time of the Ontong–Java flood basalt event: a large, actively subducting plate, a small, passive plate for which subduction has not yet begun, and a source of hot material being delivered to the base of the passive plate.

We consider a 2D, cartesian model of the mantle as a highly viscous fluid atop of which are two rigid surface plates (Fig. 2). The large, right plate actively moves toward the right at a specified velocity V_R . The smaller, left plate is subjected to a force F_L pulling to the left but is otherwise free to react to any mantle tractions induced by the motion of the right plate. The force F_L on the smaller plate is too weak to overcome the fluid tractions induced by the motions of the large plate. So the left plate is either stationary with speed $V_L = 0$ or moving slowly to the right ($V_L > 0$); if $F_L = 0$ then the left plate is entirely passive. Since the force is either zero (no incipient subduction) or pulling to the left, the boundary between the two plates is a spreading zone.

The right plate with velocity V_R is analogous to an active plate with a subducting slab connected to it. The slab is assumed to dominate the plate's motion and the prescribed velocity can be thought of as arising from the balance between the buoyancy force of the slab and viscous drag on the slab. This force balance is more or less independent of what happens to the part of the plate floating on the surface.

The left plate is analogous to a passively moving plate which is assumed not to possess a developed slab. Edge forces that act to initiate subduction are present on the passive plate; however, mantle tractions induced by the motion of the active plate overwhelm these subduction-initiating forces. The small plate is thus pulled passively along behind the large, active plate. Although both plates may initially be moving, we specify (in order to minimize the number of parameters needed in the model) that their margin does not migrate. This means that the plates are modeled like conveyor belts, the bottom sides of which are immersed in the mantle fluid.

Into the circulation described above, we introduce a starting plume head by applying a hot patch to the bottom boundary. A plume head rapidly forms and rises through the mantle to the bottom of the passive plate. Since the mantle fluid has a strongly temperature-dependent viscosity, the low-viscosity plume head (if large enough and/or of low enough viscosity) can act as a lubricant and decouple the passive plate from the mantle tractions induced by the active plate. This differs from previous experimental [20] and numerical [21–23] studies which focused on the behavior of plumes under moving plates in that here, the plume is permitted to affect the motion (i.e., the spreading rate) of the plates.

3. Modeling details

To study plate decoupling via the arrival of a hot, low-viscosity plume head beneath the plates, we employ a numerical mantle convection model.

This computational model is a two-dimensional (2D) version of the 3D model used by Ogawa et al. [24] to study thermal convection with temperature-dependent viscosity in cartesian geometry. The 2D version has been benchmarked against the results of Blakenbach et al. [25] and found to be in excellent agreement.

3.1. Mathematical description

The convection model numerically solves the non-dimensional equations for conservation of mass, momentum and energy for an infinite Prandtl number ($Pr = \nu/\kappa$, ν is kinematic viscosity, κ is thermal diffusivity), Boussinesq fluid in a 2D rectangular domain:

$$\nabla \cdot \mathbf{v} = 0 \tag{1}$$

$$0 = -\nabla P + Ra T \hat{\mathbf{k}} + \nabla \cdot [\mu(\nabla \mathbf{v} + \{\nabla \mathbf{v}\}^T)] \tag{2}$$

$$\frac{\partial T}{\partial t} + \mathbf{v} \cdot \nabla T = \nabla^2 T \tag{3}$$

where \mathbf{v} is the fluid velocity vector, P is the non-hydrostatic pressure, T is the temperature, μ is the dynamic viscosity, t is time, $\hat{\mathbf{k}}$ is the vertical unit vector, and $\{\}^T$ is a tensor transpose operator. Non-dimensionalization is achieved using the temperature difference ΔT between the cold upper surface and the hot starting plume, the thickness d of the layer, the thermal diffusion time d^2/κ , and the viscosity μ_o of the background mantle (parameter values can be found in Table 1). These parameters also help define the Rayleigh number Ra , a dimensionless measure of

convective vigor

$$Ra = \frac{\rho g \alpha \Delta T d^3}{\kappa \mu_o} \tag{4}$$

where ρ is density, g is gravitational acceleration, and α is the coefficient of thermal expansion. Although we do not consider fully developed cellular convection, Ra remains useful as a means of characterizing the strength of the plume.

In order to make best use of computational resources while examining a sufficiently large range of parameters, Ra is held fixed at 10^6 in the calculations that follow. In order to do this, one parameter in Eq. 4 must be allowed to vary; we choose the mantle viscosity μ_o as our free parameter. In order to maintain $Ra = 10^6$ given reasonable values for the other parameters (see Table 1), mantle viscosity must have the dimensional value $\mu_o = 3 \times 10^{22}$ Pa s. This viscosity is likely an order of magnitude larger than actual mantle viscosities [26–28]. Possible ramifications for such a choice are discussed in the final section.

Without loss of generality, the requirement of constant fluid properties made in the standard Boussinesq approximation is relaxed to allow for a nonuniform viscosity. The dimensionless dynamic viscosity μ is allowed to vary with temperature following an Arrhenius law of the form

$$\mu = \exp \left[E \left(\frac{1}{T+1} - 1 \right) \right] \tag{5}$$

where E is an activation parameter that determines the degree of viscosity variation. The viscosity contrast $r_\mu = \mu_{\max}/\mu_{\min}$ represents how many times more viscous the background mantle is compared to the initial viscosity of the plume and can

Table 1
Dimensional parameter values

Parameter	Symbol	Value
Mantle density	ρ	3700 kg m ⁻³
Mantle thickness	d	2900 km
Thermal diffusivity	κ	10 ⁻⁶ m ² s ⁻¹
Acceleration of gravity	g	10 m s ⁻²
Coefficient of thermal expansion	α	3 × 10 ⁻⁵ K ⁻¹
Reference temperature	T_o	1600 K
Hot-patch temperature excess	ΔT	1100 K
Maximum mantle viscosity ^a	μ_o	3 × 10 ²² Pa s

^a Mantle viscosity is chosen such that $Ra = 10^6$ for the tabulated values of the other parameters in Eq. 4.

be determined from the activation parameter via $E = 2 \ln(r_\mu)$.

The calculation domain is a 4×1 , 2D cartesian box. Since we are interested solely in the dynamics of a thermal plume interacting with surface plates and not full-scale convection in the mantle, the mantle is assumed to be isothermal at the reference temperature T_0 (for which the non-dimensional value is 0). Insulating, stress-free, impermeable boundary conditions are applied to the side-walls such that

$$\frac{\partial T}{\partial x} = \frac{\partial w}{\partial x} = u = 0 \text{ at } x = 0 \text{ and } x = 4 \quad (6)$$

while the bottom boundary is taken to be impermeable, stress-free and isothermal (except for the hot patch used to initiate the starting plume)

$$\frac{\partial u}{\partial z} = w = T = 0 \text{ at } z = 0 \quad (7)$$

The top boundary is isothermal and impermeable

$$T = w = 0 \text{ at } z = 1 \quad (8)$$

Here x and z are the horizontal and vertical coordinates and u and w are the horizontal and vertical components of the velocity vector.

The hot, low-viscosity plume is initiated using a hot patch placed on the bottom boundary. The hot patch is centered at $x = x_p$ such that $0 \leq x_p \leq x_m$, where x_m indicates the location of the margin between the two plates. The non-dimensional hot-patch temperature is defined such that

$$T(x, 0) = 1 \text{ for } (x_p - \delta_p) < x < (x_p + \delta_p) \quad (9)$$

where δ_p is the half-width of the hot patch. We choose x_p to be at the center of the passive plate in order to minimize the effects of plume-induced flow. By centering the plume beneath the passive

plate, the left-moving and right-moving limbs of the upwelling afford some degree of cancellation of induced tractions.

The horizontal velocity boundary condition at the upper surface is somewhat different from that of a simple convection model. In order to simulate two plates, one active and one passive, we define the left plate (extending from $x = 0$ to $x = x_m$) to be the passive plate and the right plate (from $x = x_m$ to $x = 4$) to be the active plate. The active plate is taken to be rigid (no-slip) with a fixed, uniform velocity $u = V_R$. The passive plate is rigid as well and is also specified to have a uniform (but unknown) velocity $u = V_L$. In order that the stresses at the base of the plates be finite, we require an analytically differentiable plate margin [29], such that

$$u(x, 1) = \frac{V_L}{2} \left[1 - \tanh \left(\frac{x - x_m}{\delta_m} \right) \right] + \frac{V_R}{2} \left[1 + \tanh \left(\frac{x - x_m}{\delta_m} \right) \right] \quad (10)$$

where δ_m is some arbitrary and small margin half-width ($\delta_m \approx 100$ km for the calculations that follow, maintaining a minimum of three grid points across the margin). The geometry and boundary conditions are shown in schematic form in Fig. 3.

Although the active-plate velocity is fixed at V_R , the passive-plate velocity V_L is not fixed. Instead, V_L depends on the combined forces acting on the passive plate, i.e., V_L is determined from a balance of the net (integrated) mantle traction forces f and the external forces F_L applied to the passive plate. Here, F_L is an end-load applied at $x = 0$ and is analogous to the incipient subduction at the northern boundary of the Izanagi plate as discussed above in Section 1.

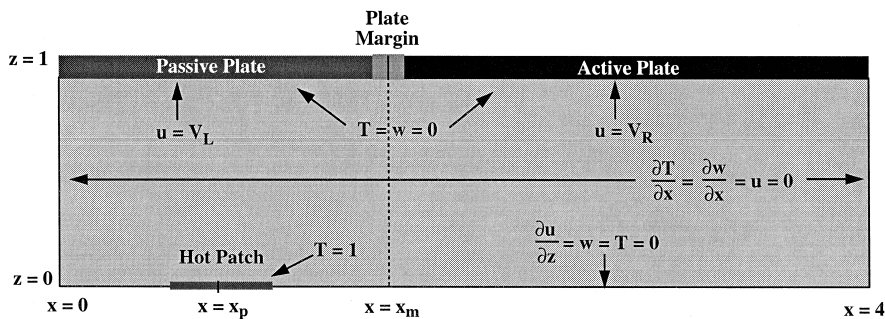


Fig. 3. Schematic diagram of the model geometry and boundary conditions.

3.2. Calculation procedure

The numerical model solves Eqs. 1–3 subject to the boundary conditions Eqs. 6–10 using an iterative relaxation procedure based on the SIMPLER algorithm [30]. A finite-volume discretization is used in which the calculation domain is divided into $N_x = 80$ and $N_z = 40$ nonuniformly spaced control volumes in the horizontal and vertical directions, respectively. A second-order accurate, unconditionally stable Crank–Nicolson scheme is used to advance the solution in time. The nonlinear coupling between Eqs. 1–3 is treated by performing several relaxation iterations during each time-step. A simple Newton–Raphson iteration is employed to obtain the updated value of V_L [31,32] within each relaxation iteration.

The net mantle traction force f on the left plate is given by [33,34]

$$f = - \int_0^{x_m} \left[\mu \frac{\partial u}{\partial z} \right]_{z=1} dx \quad (11)$$

(in which the negative sign before the integral indicates that the stress field is acting on the *bottom surface* of the passive plate having unit-normal facing downward). The applied force F_L is intended to mimic a ‘slab-pull’ force on the passive plate, perhaps brought about by incipient subduction. The acceleration of the left plate is assumed negligible (i.e., it is in dynamic equilibrium) so that these two forces balance, and we can determine the passive-plate velocity V_L which satisfies $F = F_L + f(V_L) = 0$.

We seek, via the Newton–Raphson iteration, a value of V_L for which $F = 0$. In particular, if for our initial estimate of V_L we have

$$F = F(V_L) \neq 0 \quad (12)$$

we then want a correction to V_L , call it δV_L , which gives $F = 0$. As a first approximation, we choose

$$F(V_L + \delta V_L) \approx F(V_L) + \delta V_L F'(V_L) \approx 0 \quad (13)$$

which leads to an initial estimate of δV_L of

$$\delta V_L \approx -F(V_L)/F'(V_L) \quad (14)$$

To obtain F' , the derivative of F with respect to V_L , we first calculate F with V_L and again with $V_L + dV_L$, where dV_L is some arbitrary but small perturbation to V_L . We may then calculate an estimate

of $F'(V_L)$. We correct V_L with δV_L and repeat until the Newton–Raphson iteration converges within some specified tolerance.

The iterative procedure that occurs within a single time-step is summarized by the following steps: (1) solve Eq. 3 for T using the most recent values of u and w ; (2) evaluate Eq. 5 to find μ based on the new T ; (3) solve Eq. 2 for u and w using the previous value of V_L and the most recent values of T and μ ; (4) calculate mantle tractions from Eq. 11 and determine the new V_L via Newton–Raphson iterations, Eqs. 12–14; (5) repeat until convergence is attained.

A time-step is considered converged when the maximum divergence of velocity ($\nabla \cdot \mathbf{v}$) and the Euclidean norms of the temperature and pressure residuals fall below 10^{-6} .

Initial conditions for a plate–plume interaction calculation are obtained by first solving the driven-lid problem with the hot patch turned off, i.e., without a plume. Once this flow attains steady-state, the hot patch is switched on and a thermal plume immediately forms.

4. Results

Below we present results of several numerical calculations which examine the plausibility of a reorganization of tectonic plate motions brought about by the interaction of a hot, low-viscosity plume head with the bases of tectonic plates. These calculations indicate that plate motions can be influenced by the lubricating effects of mantle plumes even to the point of causing a reversal of the direction of motion. The results, determined with fixed aspect ratio (length to depth) $a = 4$ and fixed Rayleigh number $Ra = 10^6$ (implying a background mantle viscosity of $\mu = 3 \times 10^{22}$ Pa s, as per Table 1), were found to depend on three parameters: the strength of the viscosity variation r_μ , the size of the applied end-force F_L , and the speed of the active plate V_R .

A starting plume can initiate a shift in plate motions by lubricating the base of the plates. The effectiveness of this lubrication depends on the degree of viscosity contrast r_μ between the plume and the background mantle. Where r_μ is the ratio of maximum (background mantle) to minimum (plume

source) viscosity in the system. We examine how r_μ affects decoupling of the plates by performing several calculations with an active-plate speed of $V_R = 55 \text{ mm year}^{-1}$ for different values of r_μ .

Although the model viscosity is higher than that of the mantle, we retain realistic values of driving plate speed because it is necessary to minimize the effects of flow generated by the rising plume. Since the 2D plume in our model is actually a rising sheet and not a cylindrical conduit, flow induced by the 2D plume will contribute to the motion of the passive plate more than a similar plume in 3D. Using observed plate speeds with higher than inferred mantle viscosities ensures that plate-induced mantle tractions will dominate over plume-induced tractions. Scaling V_R to be consistent with the higher mantle viscosity (or for that matter using realistic values of both V_R and μ_o in 2D cartesian geometry) would result in plume tractions comparable in size to plate tractions.

The value of F_L used is that which exactly balances the induced traction forces in Eq. 11 with no thermal plume and the passive-plate speed fixed at $V_L = 0$. For $Ra = 10^6$ and $V_R = 55 \text{ mm year}^{-1}$ this value is $F_L = 24 \times 10^{13} \text{ N m}^{-1}$. After determining F_L , the passive plate is permitted to move freely and the hot patch on the lower boundary is activated. Since F_L initially balances the traction forces due to the active plate, the passive plate begins at rest ($V_L = 0$) and any subsequent motion of the passive plate is due entirely to the effects of the mantle plume.

Time-series of the speed of the passive plate with different viscosity contrasts are shown in Fig. 4. Viscosity variation ranges from $r_\mu = 1$ (isoviscous) to $r_\mu = 10^4$. The figure clearly shows that no reversal of plate motion occurs with constant viscosity but that even a relatively small viscosity contrast ($r_\mu = 100$) provides sufficient lubrication to permit the applied end-force to overcome the mantle tractions induced on the passive plate by the active plate. Reversals of the direction of plate motion, which correspond to increases in the rate of spreading, are the result. At the largest r_μ , the speed of the passive plate changes by about 3–4 mm year^{-1} over a time-scale of about 160 million years. Recall that mantle viscosity in the model is a factor of 30 larger than what is expected for the actual mantle and despite attempts to

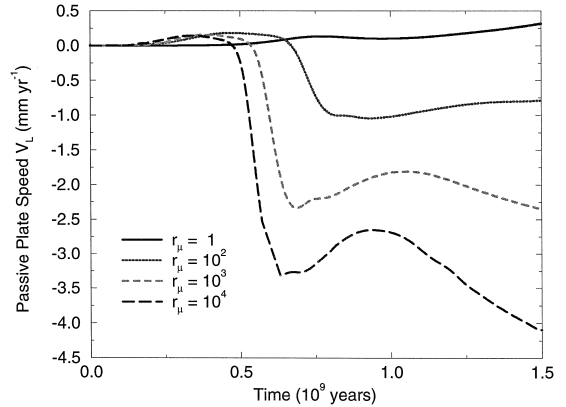


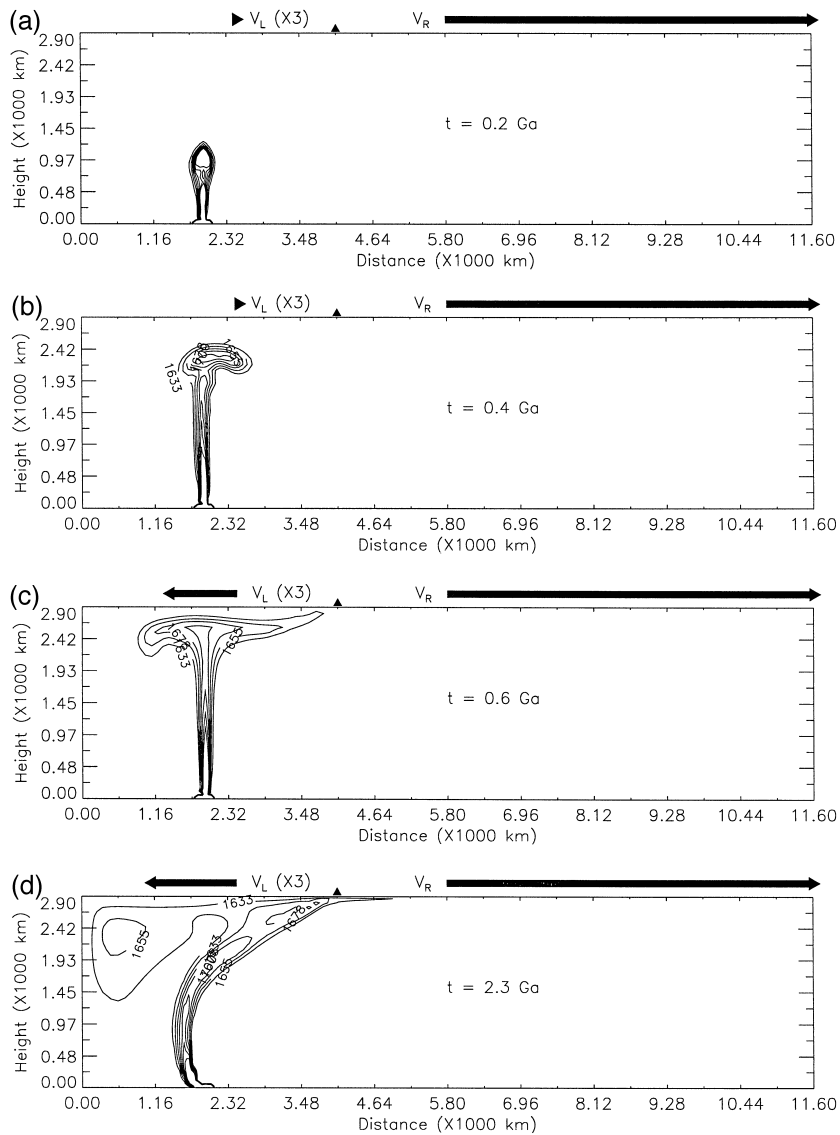
Fig. 4. Time-series of passive-plate velocity V_L for different values of viscosity contrast r_μ . $Ra = 10^6$ and $V_R = 55 \text{ mm year}^{-1}$.

minimize plume-induced tractions, the asymmetry of the plume flow (see the bottom panel of Fig. 5, for example) does exert some force on the passive plate.

Snapshots of the evolution of the plume and the reversal of the passive plate are shown in Fig. 5. These snapshots illustrate how the rising plume head undercoats the passive plate with hot, low-viscosity material. This lubrication allows decoupling of the passive plate from the mantle tractions induced by the motion of the active plate.

While some form of lubrication is required to decouple the plates, clearly, if there is no force acting to resist the induced mantle tractions or if these forces are too small, no reversal of plate motion will occur. Calculations in which r_μ and V_R are fixed but F_L is varied indicate the sensitivity of the passive-plate motion to the applied end-load. Since F_L is allowed to vary, the passive plate is no longer required to be motionless prior to plume initiation. Time-series of the passive-plate speed are shown in Fig. 6, where $r_\mu = 10^3$, $V_R = 55 \text{ mm year}^{-1}$ and F_L varies from 0 to $30 \times 10^{13} \text{ N m}^{-1}$. In each case, the arrival of the hot, low-viscosity plume head at the base of the passive plate causes some change in the spreading rate. However, only for applied end-loads greater than $\sim 20 \times 10^{13} \text{ N m}^{-1}$ does complete reversal of the direction of the passive-plate motion occur.

The behavior of the active plate, via induced mantle tractions, also exerts some influence over the motion of the passive plate. The active-plate speed



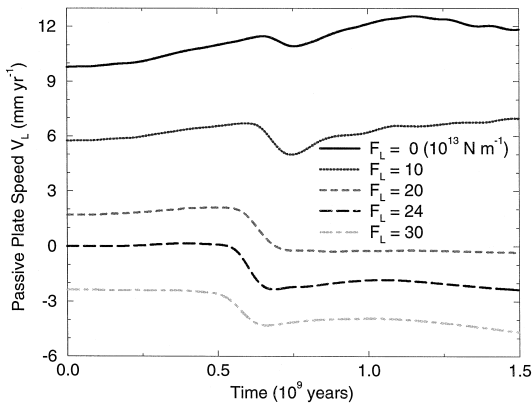


Fig. 6. Time-series of passive-plate velocity V_L for different values of applied end-load F_L . $V_R = 55 \text{ mm year}^{-1}$ and $r_\mu = 10^3$.

ing plume head model of flood basalt events can explain the correlation between flood basalts and reorganizations of plate motions if the viscosity is allowed to vary with temperature. The lubrication of plates by a hot, low-viscosity mantle diapir offers a plausible mechanism for initiating plate reversals in geologically brief periods of time.

The motion of the active plate induces mantle flow, which in turn induces mantle tractions on the passive plate. These tractions tend to drag the passive plate in the direction of the active-plate's motion. Edge forces applied to the passive plate, such as those due to incipient subduction, can act to resist these mantle tractions but are typically insufficient to cause reversals in plate motion by themselves. A mantle plume delivering hot, low-viscosity material

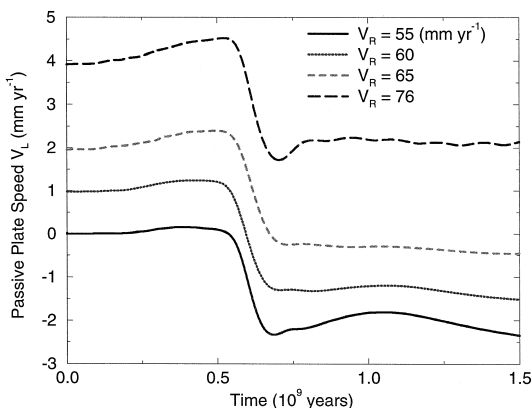


Fig. 7. Time-series of passive-plate velocity V_L for different values of active-plate speed V_R .

to the bases of the plates, serves as a lubricating mechanism which, in concert with the applied end-loads, acts to reverse the direction of the passive plate.

The three most important parameters in this model governing whether plate motions are influenced by the arrival of a mantle plume are the viscosity contrast r_μ , the magnitude of the applied end-forces F_L on the passive plate (due perhaps, to incipient subduction) and the velocity V_R of the active, driving plate. Plumes with maximum viscosity contrasts as small as $r_\mu = 100$ (for $F_L = 24 \times 10^{13} \text{ N m}^{-1}$ and $V_R = 55 \text{ mm year}^{-1}$) are sufficient to initiate reversals of plate motion. Such a result indicates the importance of including temperature-dependent rheology in geodynamic models dealing with plate-plume interactions.

Applied end-loads of around $F_L = 20 \times 10^{13} \text{ N m}^{-1}$ or more are required to initiate a change in the direction of plate motion when $r_\mu = 10^3$ and $V_R = 55 \text{ mm year}^{-1}$. Such values of F_L are somewhat larger than other estimates of plate forces [35,36] but the differences are understandable considering that in order to maintain a tractable Rayleigh number, we use a mantle viscosity that is a factor of 30 too large (see Table 1). Passive-plate reversals occur for driving-plate speeds of $V_R = 65 \text{ mm year}^{-1}$ or less (with $F_L = 24 \times 10^{13} \text{ N m}^{-1}$ and $r_\mu = 10^3$). With values of $r_\mu = 10^4$, $F_L = 24 \times 10^{13} \text{ N m}^{-1}$, and $V_R \leq 55 \text{ mm year}^{-1}$, this model predicts plate reversals with changes in plate speeds on the order of 4 mm year^{-1} over time-scales of about 160 million years.

We can speculate that with a realistic viscosity (i.e., 30 times less than the model value employed), the changes in plate speed might be closer to $\sim 100 \text{ mm year}^{-1}$ and occur over only a few (≤ 5) million years, more in line with observations. In fact, simpler models in which the low-viscosity fluid undercoating the passive plate is emplaced a priori (i.e., not delivered by a plume) show this to be the case. Passive-plate speeds (for a fixed F_L and V_R) reach realistic values when viscosity contrasts are on the order of a few hundred. Full plume simulations using a mantle viscosity of $6 \times 10^{21} \text{ Pa s}$ and applied end-loads of $5.6 \times 10^{13} \text{ N m}^{-1}$ also show that changes in plate speed occur over shorter time-scales but in these cases the fluid tractions induced by the plume

flow exert an unrealistically large influence over the motions of the passive plate.

Of course, these results are somewhat model-dependent, and the model employs assumptions that are over-simplified for actual mantle conditions. The plates themselves are approximated by a kinematic boundary condition that does not include the effect of thickening of the plate with age (i.e., cooling induces an additional force on the plate acting to initiate subduction). The temperature structure of the mantle is assumed to be isothermal in order to isolate the lubricating properties of the plume. The viscosity structure of the mantle is also neglected; the presence of a low-viscosity asthenosphere would offer an additional source of plate lubrication for which we do not account. By neglecting the endothermic phase change at 660 km, our model underestimates the temperature of the plume material since the release of latent heat during the phase change can result in 50–100 K of temperature increase [37]. In addition, partial melting, which is neglected in this model, will occur as the plume head nears the bottom of the lithosphere (small degrees of partial melting would reduce the viscosity [38] but extensive partial melting and subsequent rapid melt removal might act to increase the viscosity of the residual plume material). Fortunately, all of these factors and processes, if included in the model, would only enhance the ability of a mantle plume to initiate large-scale reorganization of plate motions. That is, each case involves either an additional source of lubrication or an increase in the applied end-force.

Conversely, there are other factors which, if included, would act to hamper a mantle plume's ability to initiate reversals of plate motions. In the model, the positions of the plates are held fixed with respect to the position of the mantle plume source. A moving plume source and/or migrating plate margins will affect the operation of this mechanism; the timing of the plume arrival becomes important. In addition, the material phase change that occurs around the 660 km seismic discontinuity will inhibit the motion of the newly subducting slab portion of the passive plate (thereby reducing the applied end-load).

Probably the most drastic over-simplification in the current model is the assumption of two-dimensionality. In 2D cartesian geometry, the mantle plume is not a cylindrical conduit but is instead an up-

welling sheet of infinite extent in one horizontal direction. A 3D plume, however, would have only a limited horizontal extent. This smaller area of contact with respect to the size of the lithospheric plate will significantly reduce the amount of lubrication applied to the base of the plate by the mantle plume. It is certainly possible for a 3D plume head to supply a great deal of lubrication to the ridge-axis but this lubrication will be concentrated in a very narrow region. So, it is not clear that a single mantle plume, even with added lubrication from the reversal enhancing factors listed above, will be sufficient to overcome the tractions induced by an actively subducting plate. The 2D plume also results in excessive plume-induced mantle tractions, although we have reduced the importance of these with respect to plate-induced tractions as discussed earlier. Finally, the 2D geometry precludes the generation of toroidal motion, an important component of actual plate motion on the earth. Models of 3D convection with surface plates have shown that the incorporation of the plates themselves into the flow can generate some toroidal flow [33]; when viscous heating is combined with temperature-dependent viscosity, plumes can excite localized toroidal motion [39].

Nevertheless, assuming that our model captures the relevant physics, these 2D calculations suggest that the lubricating mechanism is a plausible one. Mantle plume heads with temperature-dependent viscosity, in addition to delivering hot material to engender flood basalts, also have the potential to trigger reorganizations of plate motions (even to the extent of reversing the direction of motion). This mechanism offers a possible explanation of why shifts in plate motion are correlated with flood basalt events.

Acknowledgements

The research was supported by grant NAGW 2086 from the NASA Planetary Geology and Geophysics Program and Grant EAR93-03402 from the National Science Foundation. The authors would like to thank M.A. Richards, C. Lithgow-Bertelloni and an anonymous reviewer for thoughtful reviews that led to an improved paper. [RV]

References

- [1] R.S. White, D.P. McKenzie, Magmatism at rift zones: the generation of volcanic continental margins and flood basalts, *J. Geophys. Res.* 94 (1989) 7685–7729.
- [2] M.A. Richards, R.A. Duncan, V.E. Courtillot, Flood basalts and hot-spot traces: plume heads and tails, *Science* 246 (1989) 103–107.
- [3] I.H. Campbell, R.W. Griffiths, Implications of mantle plume structure for the evolution of flood basalts, *Earth Planet. Sci. Lett.* 99 (1990) 79–93.
- [4] C.G. Farnetani, M.A. Richards, Numerical investigations of the mantle plume initiation model for flood basalt events, *J. Geophys. Res.* 99 (7) (1994) 13813–13833.
- [5] D.A. Bercovici, J. Mahoney, Double flood basalts and plume head separation at the 660-kilometer discontinuity, *Science* 266 (5189) (1994) 1367–1369.
- [6] J. Skilbeck, J. Whitehead, J.A., Formation of discrete islands in linear island chains, *Nature* 272 (1978).
- [7] K. Petronotis, D. Jurdy, Pacific plate reconstructions and uncertainties, in: W.W. Sager (Ed.), *Paleomagnetic Constraints on Crustal Models*, *Tectonophysics* 182 (1990) 383–391.
- [8] T. Atwater, J. Sclater, D. Sandwell, J. Severinghaus, M.S. Marlow, Fracture zone traces across the North Pacific Cretaceous quiet zone and their tectonic implications, in: M.S. Pringle, W.W. Sager, W.V. Sliter, S. Stein (Eds.), *The Mesozoic Pacific: Geology, Tectonics and Volcanism*, *AGU, Geophys. Monogr.* 77 (1993) 137–154.
- [9] G.D. Acton, R.G. Gordon, Paleomagnetic tests of Pacific plate reconstructions and implications for motion between hotspots, *Science* 263 (1994) 1246–1254.
- [10] S.C. Cande, C.A. Raymond, J. Stock, W.F. Haxby, Geophysics of the Pitman fracture zone and Pacific–Antarctic plate motions, *Science* 270 (1995) 947–953.
- [11] D.C. Engebretson, A. Cox, R.G. Gordon, Relative motions between oceanic and continental plates in the Pacific basin, *Geol. Soc. Am. Spec. Pap.* 206 (1985).
- [12] C.R. Scotese, L.M. Gahagan, R.L. Larson, Plate tectonic reconstructions of the Cretaceous and Cenozoic ocean basins, *Tectonophysics* 155 (1988) 27–48.
- [13] R.L. Larson, M.B. Steiner, E. Erba, Y. Lancelot, Paleolatitudes and tectonic reconstructions of the oldest portion of the Pacific plate: A comparative study, *Proc. ODP, Sci. Results* 129 (1992) 615–631.
- [14] J.M. Mattinson, D.L. Kimbrough, J.Y. Bradshaw, Western Fiordland orthogneiss: Early Cretaceous arc magmatism and granulite facies metamorphism, *New Zealand, Contrib. Mineral. Petrol.* 92 (1986) 383–392.
- [15] M.C. Blake, R.N. Brothers, M.A. Lanphere, Radiometric ages of blueschists in New Caledonia, in: *International Symposium on Geodynamics in South-West Pacific*, Noumea (New Caledonia), Editions Technip, Paris, 1977.
- [16] M. Hashimoto, Introduction, in: M. Hashimoto (Ed.), *Geology of Japan, Developments in Earth and Planetary Sciences*, Terra Scientific, Tokyo, 1991.
- [17] S. Ishihara, Granites and rhyolites, in: M. Hashimoto (Ed.), *Geology of Japan, Developments in Earth and Planetary Sciences*, Terra Scientific, Tokyo, 1991.
- [18] T. Kimura, I. Hayami, S. Yoshida, *Geology of Japan*, University of Tokyo Press, Tokyo, 1991.
- [19] J.A. Tarduno, W.W. Sagar, Polar standstill of the mid-Cretaceous Pacific plate and its geodynamic implications, *Science* 269 (1995) 956–959.
- [20] M.A. Feighner, M.A. Richards, The fluid dynamics of plume–ridge and plume–plate interactions; an experimental investigation, *Earth Planet. Sci. Lett.* 129 (1–4) (1995) 171–182.
- [21] N.M. Ribe, U.R. Christensen, Three-dimensional modeling of plume–lithosphere interaction, *J. Geophys. Res.* 99 (1) (1994) 669–682.
- [22] N.M. Ribe, U.R. Christensen, J. Theissing, The dynamics of plume–ridge interaction; 1, ridge-centered plumes, *Earth Planet. Sci. Lett.* 134 (1–2) (1995) 155–168.
- [23] M.A. Feighner, L.H. Kellogg, B.J. Travis, Numerical modeling of chemically buoyant plumes at spreading ridges, *Geophys. Res. Lett.* 22 (6) (1995) 715–718.
- [24] M. Ogawa, G. Schubert, A. Zebib, Numerical simulations of three-dimensional thermal convection in a fluid with strongly temperature-dependent viscosity, *J. Fluid Mech.* 233 (1991) 299–328.
- [25] B. Blankenbach, F. Busse, U. Christensen, L. Cserepes, D. Gunkel, U. Hansen, H. Harder, G. Jarvis, M. Koch, G. Marquart, D. Moore, P. Olson, H. Schmeling, T. Schnaubelt, A benchmark comparison for mantle convection codes, *Geophys. J. Int.* 98 (1989) 23–38.
- [26] W.C. Peltier, Mantle viscosity, in: W.R. Peltier (Ed.), *Mantle Convection: Plate Tectonics and Global Dynamics*, Gordon and Breach, New York, 1989, pp. 389–478.
- [27] S.D. King, The viscosity structure of the mantle, *Rev. Geophys.* 33 (1995) 11–17.
- [28] A.M. Forte, J.X. Mitrovica, New inferences of mantle viscosity from joint inversion of long-wavelength mantle convection and post-glacial rebound data, *Geophys. Res. Lett.* 23 (1996) 1147–1150.
- [29] D. Bercovici, P. Wessel, A continuous kinematic model of plate-tectonic motions, *Geophys. J. Int.* 119 (1994) 595–610.
- [30] S.V. Patankar, *Numerical Heat Transfer and Fluid Flow*, Hemisphere, Washington, D.C., 1980.
- [31] B.H. Hager, R.J. O’Connell, A simple global model of plate dynamics and mantle convection, *J. Geophys. Res.* 86 (1981) 4843–4867.
- [32] H.P. Bunge, M.A. Richards, The origin of large scale structure in mantle convection: effects of plate motions and viscosity stratification, *Geophys. Res. Lett.* 23 (1996) 2887–2890.
- [33] C.W. Gable, R.J. O’Connell, B.J. Travis, Convection in three dimensions with surface plates: generation of toroidal flow, *J. Geophys. Res.* 96 (1991) 8391–8405.
- [34] B. Buffett, C.W. Gable, R.J. O’Connell, Linear stability of a layered fluid with mobile surface plates, *J. Geophys. Res.* 99 (1994) 19885–19900.
- [35] R.M. Richardson, Ridge forces, absolute plate motions,

- and the intraplate stress field, *J. Geophys. Res.* 97 (1992) 11739–11748.
- [36] A. Whittaker, M.H.P. Bott, G.D. Waghorn, Stresses and plate boundary forces associated with subduction plate margins, *J. Geophys. Res.* 97 (1992) 11933–11944.
- [37] G. Schubert, C. Anderson, P. Goldman, Mantle plume interaction with an endothermic phase change, *J. Geophys. Res.* 100 (1995) 8245–8256.
- [38] R.S. Borch, H.W. Green II, Deformation of peridotite at high pressure in a new molten salt cell: comparison of traditional and homologous temperature treatments, *Phys. Earth Planet. Inter.* 55 (1989) 269–276.
- [39] S. Zhang, D.A. Yuen, Intense local toroidal motion generated by variable viscosity compressible convection in 3-D spherical-shell, *Geophys. Res. Lett.* 23 (1996) 3135–3138.